KINETICS OF THE CONDENSATION OF WATER VAPOR ON A FLAT SURFACE UNDER VACUUM CONDITIONS

P. A. Novikov and É. K. Snezhko

UDC 536.423.4

The present article gives the results of an experimental investigation of the solid-condensate distribution during the condensation of water vapor on a chilled flat surface in the transition region of pressures of the ambient medium ($10 < P < 10^3$ N/m^2).

Intensification of mass-transfer processes in the chemical, metallurgical, and foodstuffs industries is widely conducted by using vacuum-equipment designs in which the sublimation and condensation surfaces are placed in the same unit (chamber). When such equipment is operated in the transition pressure region (where the transition from viscous flow to a free molecular flow mode occurs), the solid condensate is distributed extremely nonuniformly over the cooled surface, which leads to a deterioration of heat- and mass-transfer conditions and of equipment operation as a whole. It follows from analysis of the operation of such equipment that the study of the condensate-distribution patterns is necessary both to establish the condensation mechanism and to select the optimum design for vacuum sublimation equipment.

It has now been established that the most effective units are vacuum condensers in which the vapor is condensed on a cooled external surface. The distribution of the solid condensate formed on the cooled surfaces and the rate of the condensation process depend on the operating parameters (vapor and medium pressure, condensation-surface temperature, and rate of vapor–air mixture flow in chamber) and the location of the cooled surface with respect to the subliming material, i.e., the rate of heat and mass transfer, which is characterized by the transfer constants, is a function of many variables, including the evaporator size and configuration and the condenser parameters.

For viscous and molecular–viscous vapor flow regimes, the rate of heat and mass transfer and the distribution of the condensate formed depend on the angle γ between the vapor flow direction and the perpendicular to the condenser surface. When the evaporator and condenser surfaces are parallel ($\gamma = 0$), the maximum rate of heat and mass transfer and a more uniform condensate distribution on the cooled surface occur. In this case, the vapor flow itself has a quite definite direction, so that the character of the vapor distribution on the condensation surface is governed by the angle 2φ of stream broadening over the path from the evaporator to the condenser. This angle essentially depends on the pressure of the vapor–gas mixture.

The distribution and condensation rate can be used to evaluate the efficiency of condenser operation in a single-unit vacuum apparatus. We therefore first conducted experiments to determine the condensate-distribution patterns on flat and cylindrical surfaces. We also determined the condensation rate as a function of the total pressure of the vapor–gas mixture, the partial pressure of the uncondensed gases, the condensation-surface temperature, and the relative positions of the sublimation and condensation surfaces.

We will present below only the results of our experimental investigation of the condensation kinetics of steam on a flat surface. We established the character of the solid-condensate distribution on the surface and determined the local condensation rates as a function of the pressure of the steam–gas mixture ($10 < P < 10^3$ N/m^2). The other data mentioned above will be published later. The results of the first portion of our investigation can be used in applied chemistry for studying the condensation mechanism

Institute of Heat and Mass Transfer, Academy of Sciences of the Belorussian SSR, Minsk. Translated from Inzhenerno-Fizicheskii Zhurnal, Vol. 21, No. 5, pp. 842-850, November, 1971. Original article submitted December 31, 1970.

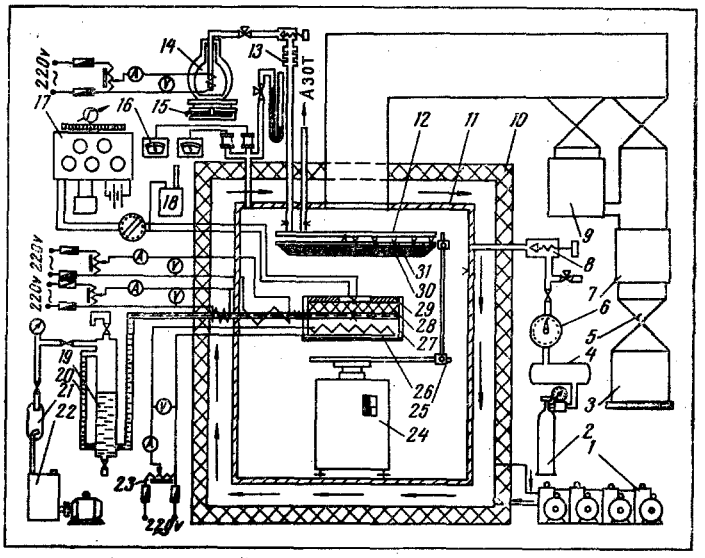

Fig. 1. Diagram of experimental apparatus: 1) condenser unit; 2) nitrogen tank; 3, 7, 9) vacuum pumps; 4) receiver; 5) vacuum traps; 6) GSB-400 gas meter; 8) regulator; 10) controlled temperature chamber; 11) pressure chamber; 12) nitrogen baffle; 13) sylphon; 14) Dewar flask (ASD-15); 15) balance; 16) thermocouple vacuum gages; 17) PMS-48 potentiometer with galvanometer; 18) container with thawing ice; 19) container with water; 20) level gage; 21) moisture settling tank; 22) pump; 23) LATR-IM220v; 24) VTK-500 balance; 25) brace; 26) heating element; 27) sublimator dish; 28) porous titanium plate; 29) adjustment ring; 30) ruler; 31) condenser disk.

during vacuum distillation and production of a number of pure organic compounds that are unstable at high temperatures and can be distilled only at low temperatures with a low vapor tension.

The experiments in this part of the investigation were conducted with the experimental apparatus shown diagramatically in Fig. 1. Within the controlled-temperature chamber (10), in which the medium temperature could be maintained and adjusted between 200 and 370°K, there was a pressure chamber fabricated from stainless steel (11), which contained all the necessary piping and an organic-glass inspection window. The condenser (31) was mounted in the horizontal plane in this chamber (on a laboratory balance with scale divisions of 0.1 g) and consisted of a thin, flat aluminum disk 0.3 mm in diameter. In order to measure the surface area of the solid condensate formed, a scale was marked on the lower surface of the disk after thorough cleaning; a thin Teflon ruler was attached to the center of the disk for the determination of the condensate profile (30).

The resultant stream of vapor moving toward the condenser under investigation was set up by sublimation of ice formed in the capillaries of a porous cermet (titanium) plate (28), which was positioned exactly coaxially with the condenser and had a sublimation surface less than the condensation surface by a factor of 100. The porous plate was contained in a flat dish, which was an evaporator with an electric heating element (26) the power of which could be adjusted. A steady-state flow was obtained by continuous delivery of distilled water to the porous plate; the density and rate of vapor flow was controlled with the amount of heat released by the evaporator heating element. The disk (condenser) was cooled and a constant temperature maintained during condensation by removal of heat through a thin gas interlayer, using a flat nitrogen-containing screen arranged coaxially with the disk.

This method permitted a more exact gravimetric study of the kinetics of water-vapor condensation under a continuous mode, even under nonsteady state transition conditions, and determination of the trend of the condensation rate (J_c) with time. Heat transfer from the disk (condenser) to the flat nitrogen screen through the thin gas interlayer was effected by thermal conduction and radiation. In order to increase the efficiency of condenser and nitrogen-screen radiation, the surfaces facing one another were coated with a

layer of carbon black; the opposite side of the screen was polished. The heat-removal method proved useful only for studying the condensation process with small thermal loads on the condenser ($q \sim 500$ W $/m^2$). For higher thermal loads, the nitrogen screen was used as the condenser, a predetermined amount of coolant (liquid or gaseous nitrogen) being pumped through it. Under steady-state conditions the coolant consumption and the coolant temperature at the screen inlet and outlet were used (taking into account all losses) to find the amount of heat evolved during condensation. The main drawback of this heat-removal method was the difficulty of continuous monitoring of the coolant delivery rate and the amount of frozen solid condensate. The evaporator, condenser, and nitrogen-screen temperatures were monitored with copper–constantan thermocouples calked into their surfaces. The sublimation rate of the ice (J_e) was determined from the amount of liquid supplied to the evaporator from the batching tank; the liquid flow rate was continuously monitored by the volumetric method, from the level in the batching-tank gage.

In order to prevent any heat flow from the walls of the pressure chamber to the condenser, the walls were held at the condenser temperature and their temperature was regulated with a three-stage Freon refrigeration apparatus and electric heaters. In order to obtain uniform heating or cooling of the pressure-chamber walls, the heat-transfer medium was circulated between the walls of the controlled-temperature and pressure chambers. The uncondensed gas was delivered from a nitrogen tank through a GSB-400 gas meter and the pressure-chamber regulator; the chamber pressure was controlled and held constant with needle valves installed in the pipe connecting the vacuum pumps. The total pressure was measured with thermocouple-type and liquid vacuum meters, while the temperature was recorded with high-sensitivity mirror galvanometers in conjuction with low-resistance potentiometers.

The basic measurements were made under steady-state conditions. Steady-state conditions were considered to have been reached when the characteristic process parameters (vaporization and condensation rates) remained unchanged in three or four measurements made over a considerable period of time.

The specific heat flux going from the evaporator through the condenser to the nitrogen screen was determined from the material-heat balance equation

$$J_c r_c = \lambda_{mix} \frac{T_c - T_s}{h} + \varepsilon\sigma(T_c^4 - T_s^4). \tag{1}$$

The conductive and radiative components of the heat flux from the condenser (disk) to the nitrogen screen were determined with the usual heat-transfer formulas for parallel plane surfaces. When the experiments were conducted under molecular–viscous conditions (the Knudsen number was $Kn > 0.01$), a correction was introduced into the formulas to take into account the temperature discontinuities at the heat-transfer surfaces. Since the condenser and screen surfaces were arranged horizontally at a short distance from one another ($h < 0.005$ m) in the rarefied atmosphere, the convective component of the thermal flux was neglected. The condensation coefficient of the water vapor was determined from the ratio of the number of molecules condensed on the flat surface to the number of molecules supplied to it, which equalled the ratio of the amount (weight) of ice formed on the condenser surface to the amount of liquid vaporized in the sublimator, i.e.,

$$\alpha_c = \frac{G_c}{G_e}. \tag{2}$$

The surface area of the condenser (flat disk) was selected in such fashion that it was covered by the solid angle of stream divergence between the sublimator and condenser.

Experiments to determine α_c were conducted under conditions where the diffusion resistance of the medium could be neglected, since it was extremely small.

The experimental data showed that, at pressures of $10 < P < 10^2$ N/m^2 and temperatures $T_c \sim 230$–240°K, the average value of α_c over the condensation surface and process time was 0.040–0.045. This is in good agreement with the theoretical value of α_c obtained for water from the Hertz–Knudsen equations [2, 3].

It was also established that the size of the solid-condensate spot formed on a flat disk (condenser) in the transition pressure region characteristic of a free molecular vapor flow mode differed little from the size of the sublimation surface. In this case, we are apparently dealing with a directional beam of vapor molecules, the density of which varies in accordance with the following rule as a function of the distance L between the sublimator and condenser:

$$J_L = J_0 \exp(-aL), \tag{3}$$

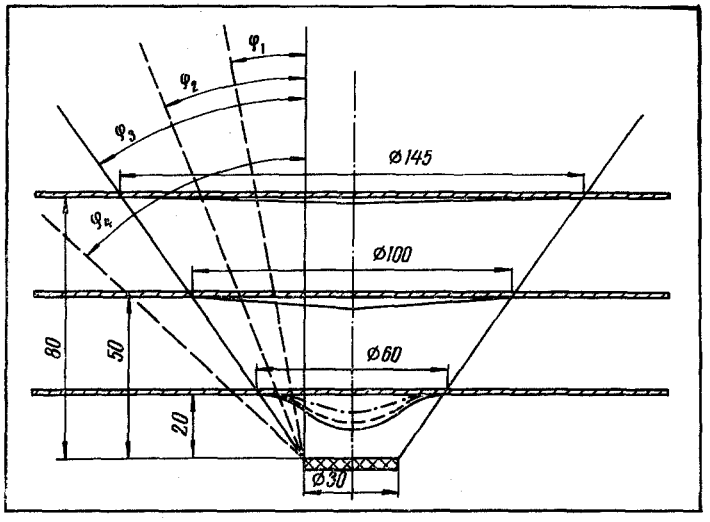

Fig. 2. Method for determination of effective dispersion angle of vapor beam (2φ) as a function of medium pressure in chamber (P) with different distances (L) between sublimator and condenser: $\varphi_1 \approx 11^\circ$ at P ~ 8 N/m^2, $\varphi_2 \approx 23^\circ$ at P ~ 60 N/m^2, $\varphi_3 \approx 36^\circ$ at P ~ 133 N/m^2, and $\varphi_4 \approx 48^\circ$ at P ~ 600 N/m^2. (The condensate profile is represented after condenser operation for 4 h by the dash line, and after 6 h by the solid line.)

where J_0 and J_L are the vapor-molecule flux densities near the sublimation surface and beyond the condenser respectively, while a is the vapor-molecule scattering factor in the beam.

It can be seen from this equation that the density of the molecular beam decreases by a factor of e for free molecular flow, where $\bar{l} = L$, $a = 1/\bar{l}$, and $aL = 1$. As the pressure is raised and $\bar{l} \ll L$, the increase in the diffusion resistance of the medium causes an increase in the dispersion of the vapor-molecule beam between the evaporator (sublimator) and the condenser. Figure 2 shows the change in the effective solid angle of vapor-beam broadening 2φ as a function of the medium pressure P_{mix} and the distance between the evaporator and condenser L. The angle φ was determined experimentally from the diameter of the ice spot formed on the chilled condenser surface. As our experiments showed, this angle is independent of the distance L but depends materially on the pressure of the vapor–gas mixture in the space between the evaporator and condenser. While $\cos\varphi$ is an exponential function of pressure, the relationship obtained by approximation to the experimental data (Fig. 3) for a viscous flow mode ($2 \cdot 10^{-1} < P_{mix}/P_0 < 1$) has the form

$$\cos\varphi = \exp\left[-k\,(P_{mix}/P_0)^{0.5}\right], \tag{4}$$

where the proportionality factor is k = 0.42; for a molecular–viscous mode ($1 \cdot 10^{-2} < P_{mix}/P_0 < 2 \cdot 10^{-1}$), we obtain

$$\cos\varphi = \exp\left[-(P_{mix}/P_0)\right]. \tag{5}$$

Thus, the beam broadening angle can be used to determine the optimum distance between the sublimator and condenser, for which the maximum heat- and mass-transfer rate is obtained.

The profile of the solid condensate formed on the plane surface depends on the duration of the condensation process, the pressure of the vapor–gas mixture, the relative positions of the sublimation and condensation surfaces, and the distance between them. At pressures P < 10 N/m^2, the interaction of the incident molecules in the vapor phase with the spontaneously evaporating molecules and complexes leads to smoothing of the condensate profile to a linear distribution.

As the pressure is raised (P $\gg$ 10 N/m^2), the number of collisions between vapor molecules and between these molecules and those of the noncondensing gas increases and the linearity of the ice distribution breaks down. With viscous or molecular–viscous flow of the vapor–gas mixture, the profile of the condensate formed is well described by a relationship of the type

TABLE 1. Values of Coefficient β Calculated from the Formula

$$\beta=0.55\left[1+\frac{L}{R_e}\left(\frac{1}{\cos^2\varphi}-1\right)^{0.5}\right]$$

$L\cdot10^2$, m	P_{mix}, N/m^2				
	33	110	200	465	665
2	0,9	1,0	1,1	1,3	1,4
5	1,4	1,75	2,0	2,45	2,7
10	2,25	3,0	3,4	4,3	4,9
15	3,1	4,2	4,8	5,7	6,5

$$y_{(R)}=y_0\exp\left[-(R^*/\beta)^2\right]. \tag{6}$$

The value of the coefficient β, which depends on the Knudsen number, is given in Table 1 ($R^*=R/R_e$).

A similar relationship was proposed at the theoretical level in Shumskii's study [1], on the basis of the Chebyshev–Gauss probability distribution rule:

$$y=\frac{A}{\frac{1}{\mathrm{Kn}}\sqrt{2\pi}}\exp\left[-\frac{x^2}{2\left(\frac{1}{\mathrm{Kn}}\right)^2}\right], \tag{7}$$

where A is a constant that depends on the characteristic dimensions of the vacuum system and Kn is the Knudsen number.

It can be seen from Eqs. (6) and (7) that the profile of the solid condensate formed on a plane surface varies from the center to the periphery in accordance with an exponential rule. The characteristics of the ice formed (structure, density, thermal conductivity, etc.) also change from the center of the condensate toward its periphery, especially at pressures close to the "triple" point. This is because capture and embedding of molecules of uncondensed gas occurs during the formation of ice layers. The farther from the center of the solid condensate, the greater the probability that molecules of uncondensed gas will enter the ice and the more porous its structure. Larger crystals are always located in the center of the solid condensate, their size and shape being governed by the temperature of the condensation surface and the pressure of the vapor–gas mixture. The vapor-molecule flux from the sublimation surface (evaporator) to the condenser (taking into account α_c) is governed by the amount of ice condensed over a definite period on the condenser (disk) surface at a definite distance L from the evaporator with a medium pressure P. Since optical methods for the determination of the vapor-stream characteristics are inapplicable in our case because of the low density of the medium and the calculation of the theoretical flux for transition modes which involve a complex process of heat and mass transfer is virtually impossible, the vapor-flux

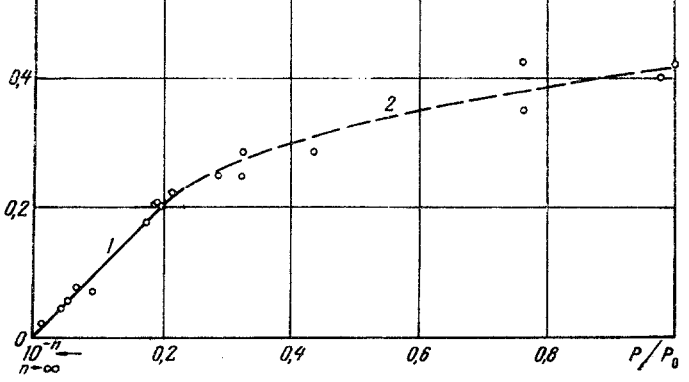

Fig. 3. Dispersion angle of vapor beam ($\cos\varphi$) as a function of pressure of vapor–air mixture (P, N/m^2), P_0 = 610 N/m^2. 1) Molecular–viscous mode; 2) viscous mode.

density at different distances from the center can be determined from the solid-condensate distribution on the condenser. It follows from this distribution that the maximum heat- and mass-transfer load occurs at the heart of the stream in the center of the spot.

If the entire condensate grows uniformly over the condensation surface, the average thickness of the condensate layer formed on a plane surface per unit time is

$$y_{av} = J_c/\rho_c. \tag{8}$$

Because of the nonuniform distribution of the average condensate-layer thickness, if we take the ratio of the volume of the condensate obtained to the area of its base $\pi\int_0^{y_0} R^2 dy/\pi R_c^2$ since the absolute amount of condensate on the surface increases with time, we find that it remains virtually constant on the corresponding surface elements. Substituting in the value of R from Eq. (6) and integrating, we obtain

$$y_{av} = y_0\left(\frac{\beta R_e}{R_c}\right)^2. \tag{9}$$

Neglecting the change in α_c and ρ_c over the condensate surface and comparing Eqs. (6), (8), and (9), we determine the local condensation rates at any radius from the center of the condensate spot $J_{c(R)}$, which are proportional to the local accretion rates $y_{(R)}$

$$J_{c(R)} = J_c (R_c/\beta R_e)^2 \exp[-(R^*/\beta)^2]. \tag{10}$$

In our case,

$$J_c = \alpha_c J_e (R_e/R_c)^2.$$

Thus,

$$J_{c(R)} = \alpha_c J_e/\beta^2 \exp[(R^*/\beta)^2]. \tag{11}$$

These relationships are applicable in the region $10 < P_{mix} < 10^3$ N/m^2.

NOTATION

β	is a characteristic of the condensate profile;
T_c, T_s	are the temperatures of the condenser surface and the nitrogen screen;
α_c, r_c	are the condensation coefficient and latent heat of condensation, respectively;
λ_{mix}, P_{mix}	are the thermal conductivity and pressure of the vapor–gas mixture;
P_0	is the pressure at the "triple" point;
J_e, J_c	are the rates of evaporation and condensation;
ρ_c	is the condensate density;
$\bar{l}$	is the average molecular free path;
y_0, $y_{(R)}$	are the condensate accretion rates at the center and at a distance R from the center of the spot;
R_e, R_c	are the radii of the evaporation and condensation surfaces;
$R^* = R/R_e$;	
L, h	are the distances from the condenser to the sublimator and to the screen, respectively.

LITERATURE CITED

1. K.P. Shumskii, Vacuum Condensers in Chemical Engineering [in Russian], Mashgiz, Moscow (1961).
2. H. Hertz, Ann. Phys., 17, 177 (1882).
3. M. Knudsen, Ann. Phys., 29, 179 (1911).